catalysts

MDPI

Review

CuS-Based Nanostructures as Catalysts for Organic Pollutants Photodegradation

Luminita Isac [1,2], Cristina Cazan [1,2], Luminita Andronic [1] and Alexandru Enesca [1,*]

[1] Product Design, Mechatronics and Environmental Department, Transilvania University of Brasov, 500036 Brasov, Romania
[2] Renewable Energy Systems and Recycling Research Center, Transilvania University of Brasov, 500036 Brasov, Romania
* Correspondence: aenesca@unitbv.ro

Abstract: The direct or indirect discharge of toxic and non-biodegradable organic pollutants into water represents a huge threat that affects human health and the environment. Therefore, the treatment of wastewater, using sustainable technologies, is absolutely necessary for reusability. Photocatalysis is considered one of the most innovative advanced techniques used for pollutant removal from wastewater, due to its high efficiency, ease of process, low-cost, and the environmentally friendly secondary compounds that occur. The key of photocatalysis technology is the careful selection of catalysts, usually semiconductor materials with high absorption capacity for solar light, and conductivity for photogenerated charge carriers. Among copper sulfides, CuS (covellite), a semiconductor with different morphologies and bandgap values, is recognized as an important photocatalyst used for the removal of organic pollutants (dyes, pesticides, pharmaceutics etc.) from wastewater. This review deals with recent developments in organic pollutant photodegradation, using as catalysts various CuS nanostructures, consisting of CuS NPs, CuS QDs, and heterojunctions (CuS/carbon-based materials, CuS/organic semiconductor, CuS/metal oxide). The effects of different synthesis parameters (Cu:S molar ratios, surfactant concentration etc.) and properties (particle size, morphology, bandgap energy, and surface properties) on the photocatalytic performance of CuS-based catalysts for the degradation of various organic pollutants are extensively discussed.

Keywords: CuS nanostructures; heterojunctions; photocatalysis; organic pollutants; wastewater treatment

Citation: Isac, L.; Cazan, C.; Andronic, L.; Enesca, A. CuS-Based Nanostructures as Catalysts for Organic Pollutants Photodegradation. *Catalysts* **2022**, *12*, 1135. https://doi.org/10.3390/catal12101135

Academic Editor: John Vakros

Received: 1 September 2022
Accepted: 25 September 2022
Published: 28 September 2022

1. Introduction

The global population growth has resulted in constantly increasing environmental pollution, with serious consequences for human health. Harmful impacts on humans, animals, and the environment are due to the water resource contamination with inorganic, i.e., heavy metals [1–3], and organic, pollutants. Toxic, non-biodegradable, and recalcitrant organic pollutants, such as dyes [4–7], pesticides [8], pharmaceutical active compounds (PhACs) [9,10], and other organic pollutants [11,12], are discharged into water from various industries: textile, leather, food, pharmaceutical, cosmetic, agriculture, plastic, etc. Consequently, the removal of these pollutants from wastewater, via appropriate technology, still remains a great challenge for worldwide researchers.

In this context, many technologies, such as sedimentation, reverse osmosis (RO), coagulation, flotation, solvent extraction, electrolysis, biodegradation, ozonation, sonolysis, sonophotocatalysis, gammaeradiolysis, photo-Fenton, photo-, electro-, and photoelectrocatalysis and chemical catalysis, and combined anaerobic photocatalysis with membrane techniques, have been developed [10,13–15]. Among these technologies, photocatalysis, an advanced oxidation process (AOP), has attracted considerable attention as a green and sustainable technology with promising prospects in global environmental issues remediation [16–18]. Although the photocatalytic degradation of organic pollutants has been

proven to have significant results, its application at the industrial level faces certain deficiencies related to the efficient use of solar energy, mainly due to the high photo-generated carriers recombination rate [19,20]. Thus, the design and development of low-cost and highly efficient catalysts is the main topic in photocatalysis research. Semiconductor materials, with wide solar selective spectral response, high activity, and increased chemical and physical stability, are the most frequently used photocatalysts. As wastewater treatment technology, semiconductor-based photocatalysis has numerous advantages, such as simplicity, ease of handling, good reproducibility, high efficiency, and low costs. Moreover, it is an ecological, non-toxic and energy-free technology [5].

An important class of semiconductor photocatalysts is that of metal sulfides. For these materials, the band gap energy can be easily tuned by simply controlling the particle size without changing the chemical composition of the metal sulfide.

Copper sulfides (Cu_xS, x = 0.5–2), one of the most significant metal chalcogenide representatives, have been intensively studied in recent decades, due to their particular properties (optical and electrical), that result from their various chemical compositions and morphologies. Considering the chemical composition (x variation), at least eight crystalline phases of Cu_xS have been reported to date, ranging from the "copper low" sulfide CuS_2 (copper disulfide, x = 0.5) to the copper-rich phase Cu_2S (chalcocite, x = 2).

Adjusting the chemical composition (x value), optoelectronic properties are modified, affecting the photocatalytic performance of Cu_xS catalyst. Generally, the increase of x causes a decrease in the Cu_xS photocatalytic activity. Copper sulfides with x = 1.8–2 act as more efficient materials for solar cells and optoelectronic devices than as photocatalysts [21–23]. Accordingly, it was reported [24] that Cu_2S NPs (0.08 g/L pollutant solution), obtained by a template free polyol reaction, degraded only 51% of dye ABRX-3B (100 mg/L) under Vis light (300W Xe lamp), after 100 min. More recently, the photocatalytic activity of Cu_2S-metal oxide(s) heterostructures, prepared by a simple two-step sol–gel procedure, was studied under UV and UV–Vis irradiation scenarios using herbicide S-MCh (30 mg/L) as the reference pollutant [25]. The results showed that the three-component heterostructure of $Cu_2S/TiO_2/WO_3$ had higher photocatalytic efficiency (61%) compared with two-component heterostructures, 30% for Cu_2S/TiO_2, and 28% for Cu_2S/WO_3, respectively, after 8 h in UV-Vis light irradiation. A lower photocatalytic efficiency (~10%) was reported for Cu_9S_5 ($Cu_{1.8}S$) MCs in the degradation of MB solution (5.8 mg/L), under Vis light irradiation, after 175 min [26].

Another potential non-stoichiometric copper sulfide catalyst is Cu_7S_4 ($Cu_{1.75}S$). However, its photocatalytic application is reduced, due to both the high recombination rate of the photogenerated electron/holes, and also to the powder recycling issues. Thus, as an efficient alternative to powders, flexible Cu mash/Cu_7S_4 films were developed via a facile in situ anodization technique [16]. Using Cu/Cu_7S_4 films of 4 cm^2 area as catalysts, the highest efficiency in the photocatalytic Fenton-like dye MB (10 mg/L) degradation was 98.4%, under simulated sunlight, after 140 min.

Over recent years, the CuS semiconductor has been shown to be a promising candidate for visible light photocatalysis, due to its narrow band gap and good optical absorption properties in the Vis-NIR region. Based on the increased photocatalytic performances of CuS, compared with Cu_xS (x = 1.8–2) and $Cu_{1.75}S$ (more efficient and more environmentally friendly as films), therefore, a large amount of research was conducted for this review, which is focused on the use of CuS nanostructured powders as photocatalysts for organic pollutant degradation in wastewater.

Due to its special properties, e.g., increased conductivity at high temperature, superconductivity at 1.6 K, (electro)chemical-sensing capabilities, low-toxicity, nonlinear optical and ideal solar energy absorption capacity, CuS shows a versatile range of applications, including solar thermal collectors [27], artificial photosynthesis [28], gas sensors [29–32], biosensors [29,33,34], photodynamic therapy of cancer [29,32,34], lithium-ion batteries [29,35], supercapacitors [29,36], photoconductors [37], water disinfection [38–41],

hydrogen production via water splitting [37,42], thermoelectric materials [29], and photocatalysis [4,37].

According to literature [10,14,43,44], the lack of chemical stability, fast recombination of photogenerated charge carriers, and particle aggregation in solution are still significant drawbacks of a single semiconductor photocatalyst, such as CuS. An effective solution to these impediments is heterojunction construction with additional advantages, such as improving solar energy absorption and carriers charge transfer rate. The photocatalytic performance of CuS nanostructures (NSs) and CuS-based hetero-nanostructures depends on particles size, surface area, morphology, and the interface properties, that can be tailored by tuning the synthesis methods and/or conditions.

In recent years, many studies have been developed on CuS NSs with applications in environmental issues, especially in wastewater treatment. In this review, the photocatalytic activity of various CuS-based nanostructures for degradation of different organic pollutants, such as organic dyes, pesticides, phenol and phenolic compounds, pharmaceutical active compounds, etc., under simulated (UV, Vis) and sunlight irradiation, is extensively discussed. This study aims to identify the photocatalytic performances of recently reported CuS-based catalysts, for possible future improvements so as to ensure it is as efficient as possible for the degradation of industrial organic pollutants in wastewater effluents. In Figure 1 is illustrated the schematic representation of this review regarding CuS-based nanostructures photocatalysts obtaining, their specific properties (morphology, band gap energy, specific surface area), and application in organic pollutants degradation from wastewater.

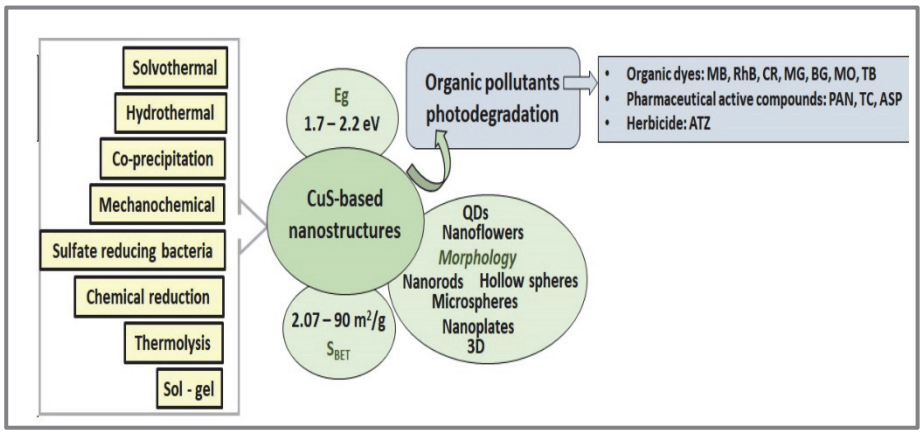

Figure 1. Synthesis methods and specific properties of CuS-based nanostructures photocatalysts used in organic pollutants degradation from wastewater.

2. CuS Nanostructures with Different Morphologies as Catalysts for Organic Pollutant Photodegradation

At room temperature, CuS (covellite) has a hexagonal crystalline structure (space group P63/mmc, a = 3.8020 Å, c = 16.430 Å) consisting of unit cells, in which layers of planar CuS_3 (triangles) and CuS_4 (tetrahedrons) with S−S bonds alternate. At 55 K, the CuS hexagonal structure changes to orthorhombic, due to second-order phase transition resulting in orthorhombic distortion of the Cu-S and S-S bond lengths [45,46].

The energy band alignments and total–partial density of states, calculated with the generalized gradient approximation (GGA) of the density functional theory, showed that CuS has significant metallic behavior due to p(S)−d(Cu) orbital interactions up to Fermi level [45]. The Fermi level, an empty energy band induced by both copper vacancy and sulfur vacancy on the top of VB, is an important factor in the evaluation of CuS photoelectronic properties, mainly related to the potential local surface plasmon resonance (LSPR) [47]. Due to its deficiency in Cu atoms (comparing with Cu_2S), CuS exhibits the highest concentration of free carriers (holes) in the VB, resulting in LSPR bands in the NIR region, hence having extended light absorption [48].

As a copper sulfides class representative, CuS is a p-type semiconductor with a bandgap energy ranging from 1.7 eV to 3.46 eV [33,49] but, for most CuS, the Eg values are in the range of 1, 7–2.2 eV. Controlling the CuS semiconductor morphology (shape and particle size), the band gap can be tailored without changing the chemical composition of the material [50]. For example, the band gap energy for CuS nanoparticles (NPs) can vary from 1.7 to 2.14 eV, depending on morphology: 1.7 eV for hollow spheres [51], 1.87 eV for nanoflowers [52], 1.97 eV for microspheres [53], 2.1 eV for nanoplates [54] and 2.12 eV for flake-like nanostructures [55].

Thus, many works have reported the preparation of CuS with different morphologies, from quantum dots (QDs) to 3D hierarchical CuS architectures consisting of 1D nanotubes, using methods such as hydrothermal [50,56,57], solvothermal [58–63], co-precipitation [64,65], photochemical precipitation [66], mechanochemical [67,68], thermolysis [49], chemical reduction [69], microwave assisted growth [70] and solid-state reaction routes [71]. However, the preparation of uniform CuS nanostructures, through simple, fast, ecological and low-cost technologies, still remains a significant challenge for all researchers in the field.

Covellite nanoparticles (CuS NPs) with remarkable chemical, structural and surface properties, significantly different from those of bulk, are considered promising photocatalytic materials [55]. The photocatalytic properties of CuS catalyst can be tailored by changing preparation method parameters. In addition, the photocatalyst dosage, the pollutant and its concentration, the type and intensity of the irradiation source are other important factors to be considered in the photodegradation process. The photocatalytic activity of CuS-based nanostructures for the degradation of different organic pollutants is selectively presented in Table 1.

Table 1. Representative studies on organic pollutants photodegradation using nanostructured CuS-based catalysts.

Catalyst	Synthesis Method	Pollutant Conc. (mg/L)	Catalyst Dosage (g/L)	Light Source	η* (%)	t (min)	Ref.
CuS NPs	ST	MB (500)	0.5–2	UV (90 W Xe lamp) Vis (160 W Hg -W lamp)	98.26 100	30	[72]
CuS NPs	ST	MB (6.4) CR (13.9) RhB (9.6) EY (13)	0.03	UV (12 W G8 T5 Philips) Vis (160 W Hg lamp) Solar	70.79, 85.13, 90.29 75.47, 63.21, 60.35 50.04, 60.37, 69.23 79.49, 56.02, 91.97	240	[61]
CuS NPs	Aqueous solution route	MB (20) MB + H_2O_2	0.1	Vis (150 W Xe arc lamp)	39 92	90	[52]
CuS NPs	Sulfate reducing bacteria (SRB)	MB (16) RhB (24) + H_2O_2	0.3–0.5	Vis (600 W halogen lamp)	94 61.2	5.5 25	[55]
CuS NPs	PVP assisted ST	MB (400) + H_2O_2	0.1	Solar	96.5	48	[53]
CuS 3D NSs	ST	MB (20) + H_2O_2	0.2	Vis (10 kW/m^2, CEL HXF 300)	90	30	[62]
CuS NPs	Solution aerosol thermolysis	MB (12.8) RhB (9.6) MO (9.8) + H_2O_2	1	Vis (300 W Xe lamp)	98 98 50	15 50 45	[27]
CuS MCs	Subcritical & supercritical methanol reaction	MB (5.8)	0.2	Vis (25 W day-light lamp)	85.4	300	[26]
CuS NPs	CoPp	RhB (20) RhB + H_2O_2	0.05	Vis (150 W Xe lamp)	99 99	120 60	[51]
CuS QDs	Mechano-chemical	RhB (10) RhB + H_2O_2	0.4	Vis (150 W Xe lamp)	60 95	30	[67]

Table 1. *Cont.*

Catalyst	Synthesis Method	Pollutant Conc. (mg/L)	Catalyst Dosage (g/L)	Light Source	η* (%)	t (min)	Ref.
CuS NPs	Mixed solvent route	RhB (50) + H_2O_2	0.2	Vis (1000 W halide lamp)	94	60	[73]
3D CuS NSs	ST & self-assembly	RhB (50) + H_2O_2	0.2	Vis (150 W Xe lamp)	99	45	[74]
3D CuS NSs	One-step in situ heating sulfuration route	MB (10) RhB (10) MB/RhB + H_2O_2	1.25	Vis (300 W xenon lamp)	99 99 99	25	[75]
CuS NPs	One pot synthesis from Cu(II) dithio-carbamate	CR (100)	0.5	Solar	100	40	[54]
CuS NPs	Solid-state reaction	MoO (60) SO (60) AO (60)	0.1	Vis (500 W Hg lamp)	51 22 45	180	[71]
3D CuS NSs	HT	4-CP (100) 4-CP + H_2O_2	1	Vis (49.700 lux)	62 83	300	[57]
CuS NPs Cu_2S NPs CuS-Cu_2S NPS	One-step HT (tuning Cu:S molar ratios)	RhB (10) + H_2O_2	0.2	Vis (250 W cold Xe lamp)	96 87 92	5	[56]
CuS-Cu_2S NPs	Chemical reduction	MB (3.2) MG (3.65) MO (3.27) MV (3.6) RhB (4.79)	0.4	Solar	61.95 90.25 9.4 85.03 70.16	100 40 180 60 80	[69]
CuS/KCC1	ST	HA (2)	0.1	UV-C (18 W lamp)	89.5	90	[76]
CuS/ZnO	HT	MB (9.6) TB (16.2)	0.7	Vis (52 W renewable household Philips LEDs)	93 87.5	16 18	[77]
$Cu_{1-x}Ag_xS$ ($0.0 \leq x \leq 0.1$)	CoPp	MB (6)	0.25	Vis (indigenous light reactor)	75.4	90	[33]
CuS/rGO	CoPp	MG (10)	0.1	Solar	99.2	90	[14]
CuS/CQDs	Carbonization of water hyacinth weed + SG (CuS)	BG (50)	0.09	Vis (200 W tungsten lamp)	96	90	[78]
CuS/CQDs	Carbonization of peanut shells + HT (CuS)	PAN (20)	0.2	Vis (400 W Hg lamp)	96.5	150	[50]
CuS/PDI	Two-step self-assembly	TC (50)	0.6	Vis (300 W Xe lamp)	90	120	[79]
CuS/rGO	SG	ATZ (50)	0.8	Vis (300 W Xe lamp)	100	20	[43]
CuS/WO_3-AC	HT	ASP (10)	-	Vis (400 W metal halide lamp)	97.6	150	[80]

η* is the efficiency degradation of pollutant after t min of irradiation.

The Vis and natural light-driven photocatalytic degradation of cationic azo dye methylene blue (MB) using CuS nanoparticles (NPs) with different morphologies, has been demonstrated to be an attractive topic for many research. Flower-like [52], hollow microspheres [53], and flake- and spherical-like CuS NPs [55], prepared by simple aqueous solution route, facile PVP assisted solvothermal process and biological sulfate reduction, were investigated as photocatalysts in the degradation of MB, in the absence/presence of H_2O_2.

The CuS nanostructured flowers, with diameters of about 800–1200 nm, Eg = 1.87 eV and BET surface areas of 61.55 m^2/g, obtained by using a simple aqueous solution route without any surfactant addition, removed only 39% MB after 90 min, under Vis light irradiation [52]. The addition of H_2O_2 in the photocatalytic system significantly increased the degradation efficiency to 92%, after the same irradiation time. This increase was due to the presence of H_2O_2 molecules, which enhanced the dye degradation by accelerating the formation of hydroxyl radicals (·OH), the active species which promote the oxidation of MB into smaller, non-toxic molecules [52,81].

An enhanced photocatalytic efficiency (94%) in the degradation of MB under natural light (sunlight), in the presence of H_2O_2, was reported for CuS hollow microspheres

mesoporous structures with a bandgap of ~1.97 eV and surface area of 36 m^2/g [53]. The CuS hollow microspheres nanostructures were obtained by the solvothermal process, varying the amounts of PVP surfactant (0–2 g), the copper/sulfur precursors, and solvents, while the precursor ratios were maintained at constant during the experiments. The average diameter of microspheres in the nanosheets-based hierarchical structure was about 2.3 µm. The studied photocatalysts showed excellent stability and recyclability, with 96.5% of the dye removed after 6th cycle. The photocatalytic performance of CuS catalyst was attributed to its hollow microsphere morphology, which favors the absorption of more MB molecules, promotes the light generated charge carriers transfer to the reactive surface and allows rapid diffusion of the reactants and products during the oxidation/reduction reaction [53].

CuS NPs with two different morphologies were synthesized via the sulfate reducing bacteria (RBS) method by changing the copper precursor concentration: lower concentrations favored the obtaining of flake-like nanoparticles (Eg = 2.12 eV) with an average width of 25 nm and average length of 130 nm, while spherical-like CuS NPs (Eg = 2.14 eV), with average diameter in the range 30–50 nm, were synthesized at higher concentrations [55].

Both the flake-like and spherical-like CuS NPS showed high photodegradation efficiency for the MB + H_2O_2 system, respectively 94% after 5.5 min and 93% after 1 min illumination with a halogen lamp (600 W). Although these photocatalysts have the advantage of being used in applications that require short irradiation time or short catalyst–pollutant contact time, their reusability is still an open-issue for further studies.

The studies mentioned above confirm that the photocatalytic activity of CuS NPs with hollow microspheres or spherical-like morphologies, with consistent shape and size of spherical particles, was higher than that of CuS NPs with non-spherical structures.

The MB dye photodegradation mechanism, through oxidation/reduction reactions, using CuS NPs as the photocatalyst, in the absence/presence of H_2O_2 molecules, is illustrated in Figure 2.

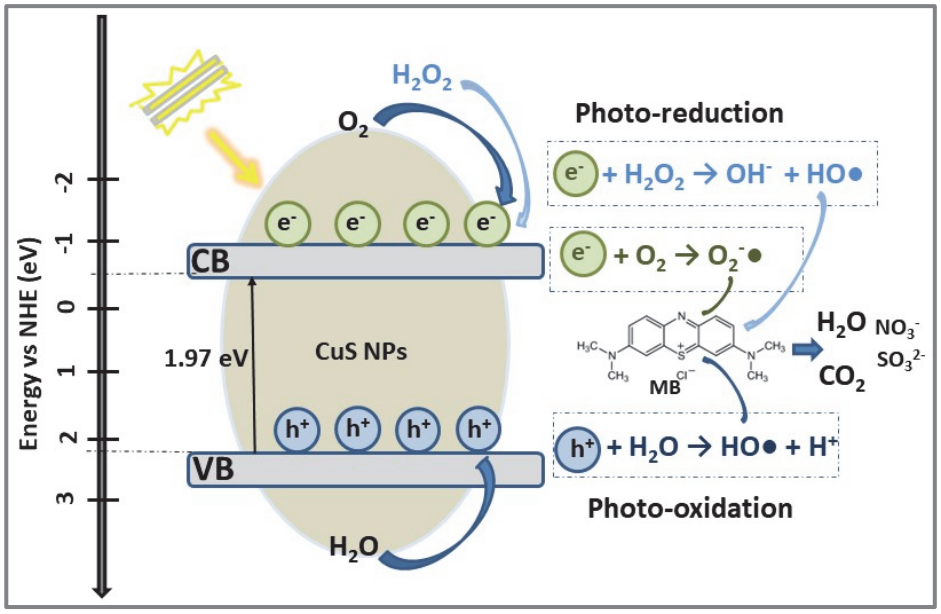

Figure 2. The photocatalytic degradation mechanism of MB dye using CuS NPs photocatalyst under sunlight irradiation.

The adsorption and photocatalysis performance of CuS nanostructures with different morphologies of particles, prepared by a simple co-precipitation method using $Cu(NO_3)_2$ and thioacetamide as precursors, for degradation of the dye Rhodamine B (RhB) aqueous solutions (20 mg/L) under Vis light irradiation (150 W Xe lamp equipped with a glass filter) were evaluated by Li and Wang [51]. It was reported that CuS NPs with different morphologies (flakes, rods and hollow spheres), and Eg = 1.7 eV had good photodegradation

efficiency for RhB, with removal rates higher than 85% within 120 min. As was expected, CuS hollow spheres, with 400–3500 nm outer diameter and 10–400 nm thickness, formed by self-assembly of nanoparticles with sizes in the range 1–2 μm, showed a RhB photodegradation of 99% in 120 min. The addition of a small amount of H_2O_2 (1mL/100 mL dye solution) had the result of halving the time necessary for photodegradation of 99% RhB with high concentration (50 mg/L) in wastewater. The increased photocatalytic activity of the CuS NPs, attributed to the combination of the adsorption and photocatalysis processes, demonstrates the potential application of CuS NPs photocatalyst in high dye concentration wastewater treatment.

The photocatalytic activity and stability of CuS QDs in degradation of RhB solutions under visible light illumination (150 W Xe lamp) were studied by Li et al. [67]. Using a low-cost and simple mechanochemical ball milling method, CuS powders containing ultrafine crystals with uniform size (1–5 nm) and an average diameter of 2.9 nm, were prepared. The calculated BET surface area of about 90.0 m^2/g, which was significantly higher than that of CuS NPs (30.6 m^2/g, [51]), was expected to improve the photocatalytic activity of the CuS QDs. Higher specific surface area, with more reactive sites and shorter migration distance, reduced the recombination rate of photogenerated electron/hole pairs. Accordingly, the H_2O_2 addition increased the degradation efficiency of RhB from about 60% to 95%, after 30 min exposure in Vis light, due to the quantum effect of CuS QDs which favors ultra-fast transfer of charge carriers from CuS QDs to RhB dye.

Based on previous studies, both CuS NPs and CuS QDs are excellent photocatalysts for RhB degradation, depending on the dye concentration in wastewater: CuS QDs is more efficient in wastewater with a low content of dye, while CuS NPs shows good efficiency in dye-concentrated wastewater as well.

3D nanostructured CuS have been remarked on as materials with high solar catalytic efficiency due to their large surface areas with sufficiently active sites, which improve CuS surface-reactants contact [62].

The hierarchical 3D CuS nanostructures, prepared by low-temperature solvothermal grow of 1D CuS nanotubes on a self-assembled 3D $Cu(MAA)_2$ precursor, not only provided the advantage of a large number of active sites on the surfaces, but also the advantages of improved molecular/ionic transport (through the 1D nanotubes), and of good mechanical stability (due to the 3D structure) [74]. The as-prepared 3D hierarchical CuS architectures showed a degradation of almost 99% of RhB within 45 min, in the presence of visible light and oxidizing agent (H_2O_2). The stability and reusability of the photocatalysts proved to be quite good, the removal rate of RhB reaching 70% after 5 cycles.

A simple and one-step in situ heating sulfuration procedure was used to prepare the CuS photocatalyst with a 3D hierarchical nanostructure with CuS nanoplates formed on the copper foam precursor structure in [75]. According to this study's results, the excellent photocatalytic performance of 3D nanostructured CuS catalyst resulting in 99% degradation of RhB + H_2O_2 solution when exposed in simulated solar light for 25 min, was attributed to the synergistic effects of high optical absorption (Eg = 1.58 eV), and large specific surface area (12.06 m_2/g), resulting in sufficient reaction active sites. Moreover, the photocatalytic activity and stability of the studied catalysts did not alter after 4 photocatalytic cycles, which made them ideal recyclable catalysts.

Cu_xS nanoparticles with different compositions (x = 1, 2) and morphologies were synthesized via simple and environmentally friendly methods, e.g., one-step hydrothermal and thermal chemical reduction of S precursor with/without surfactant, in [56,69].

By tuning the molar ratios Cu:S (1:0.1–1:3) of copper acetate and sublimed sulfur precursors in polyethylene (PEG-400) surfactant, CuS, Cu_2S, and CuS–Cu_2S NPs with various morphologies and particle sizes, and, therefore, different band gap energies, were obtained:

Cu_2S spherical and irregular nanoflakes (Eg = 3.5 eV) for Cu:S = 1:0.25
Cu_2S-CuS irregular flakes with 30 nm thickness (Eg = 2.72 eV) for Cu:S = 1:0.75
CuS irregular nanoflakes with particle sizes between 200 and 300 nm and thickness less than 30 nm (Eg = 2.01 eV) for Cu:S = 1:1.

The photocatalytic experiments showed that photocatalyst efficiency in RhB degradation under Vis light (250W cold xenon lamp with cut-off wavelength of 420 nm), in the presence of H_2O_2, increases with band gap energy decrease, thus CuS NPs degraded 96% RhB in 5 min, while Cu_2S and Cu_2S-CuS NPs degraded 87% and 92% RhB respectively [56].

The RhB photodegradation reaction mechanism in presence of CuS NPs under visible light irradiation is schematically presented in Figure 3.

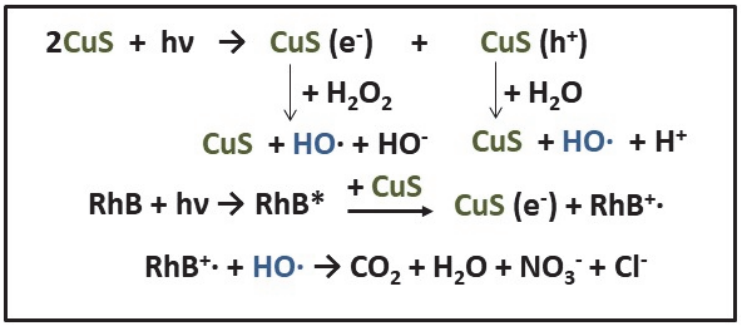

Figure 3. The reaction mechanism proposed for RhB photodegradation by CuS NPs catalyst.

When CuS photocatalyst absorbs photons from solar light or an irradiation source, with energy equal or higher than its band-gap, the electrons from CB are transferred to VB, resulting in photogenerated electrons CuS (e^-) and holes CuS (h^+). The H_2O_2 molecules capture these photogenerated electrons and rapidly generate hydroxyl radicals (HO·) and hydroxide ions (OH^-), while the photogenerated holes react with H_2O forming HO·. In the meantime, RhB dye absorbs Vis light and undergoes a transition to its excited state (RhB*), which transfers electrons to CuS, resulting in CuS(e^-) and RhB^+. Then, the highly reactive radical HO· oxidizes and decomposes RhB^+ to CO_2, H_2O and other salt ions [4,56].

Shamraiz et al. synthesized CuS–Cu_2S NPs, with an average size less than 30 nm, by chemical reduction of copper thiourea complex, without any surfactant, at moderate temperature [69]. The CuS–Cu_2S NPs were tested as photocatalysts in the degradation of different dyes under direct sunlight (outdoor lightening), without H_2O_2 addition. The results showed that the photodegradation process was faster for cationic dyes, such as MV (85.03% in 60 min), MG (90,25% in 40 min) and RhB (70.16% in 80 min), but almost negligible for the anionic dye MO (9.4% in 3 h). This behavior of the CuS–Cu_2S catalyst in cationic dye photodegradation was attributed to the presence of active negative charges (OH^-) on the catalyst surface, which were electrostatically attracted by cationic dye molecules, thus facilitating the electron transfer under direct sunlight irradiation [69].

The photocatalytic performance of CuS nanoparticles, with size < 20 nm and specific surface area of 34.37 m^2/g, in the degradation of organic dye pollutants, MB, RhB, EY and CR, under various light (UV, Vis and solar) irradiations, was evaluated by Ayodhya et al. [61]. For CuS NPs synthesis, a simple, relatively fast and green (using xanthan gum as a capping agent) solvothermal method was proposed. The photodegradation of the MB, RhB, EY and CR dyes in the absence and presence of CuS NPs were studied under similar experimental conditions, using UV, Vis and solar light sources. The photocatalytic performances of CuS NPs are shown in Figure 4.

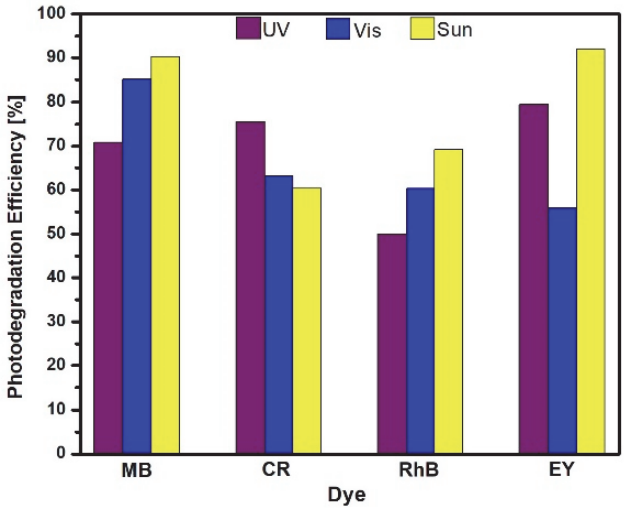

Figure 4. The photocatalytic activity of CuS NPs in dyes degradation under different light irradiations, for 4 h.

It can be observed that CuS NPs showed good photocatalytic activity for dye degradation in sunlight irradiation, ranging from 69.2% for RhB to 92% for EY. The exception was CR which degraded better in UV light (75.5% photodegradation efficiency) in the presence of CuS catalyst.

3. CuS-Based Heterostructures as Catalysts for Organic Pollutant Photodegradation

Although previous studies confirmed the successful applicability of CuS NP photocatalysts in the degradation of organic contaminants (especially organic dyes), the photocatalytic efficiency of single CuS is quite low for the complete degradation of persistent, much more toxic, organic compounds (dyes, pharmaceuticals, pesticides) from wastewater.

3.1. CuS/Carbon-Based Materials Heterostructures as Catalysts for Organic Pollutant Photodegradation

Carbon quantum dots (CQDs), with sizes under 10 nm and fluorescent properties, have large surface areas, high porosity, excellent electrical conductivity, relatively low cost and toxicity, and high aqueous stability. Due to these properties, CQDs can act as absorbents for water impurities, but also as supporting catalyst (co-catalyst) for the main photocatalyst (CuS) [50,78].

Another promising supporting catalyst for CuS is reduced graphene oxide (rGO) with high surface area, efficient electron transfer, and superior conductivity [39,52].

Therefore, the CuS/CQD and CuS/rGO composites could be attractive solutions for photocatalytic degradation of persistent organic contaminants under Vis light irradiation.

Recent investigations on the degradation of brilliant green (BG) highly toxic dye, usually used in textiles and paper industries but also in poultry feed to avoid fungi and parasite contagion, and panadol (PAN), one of the top three most commonly prescribed drugs in the world, were done using CuS/CQD photocatalysts [50,73]. In both studies, CQDs were obtained by carbonization of vegetative wastes (water hyacinth weed, peanut shells), while CuS NPs were prepared via sol–gel [78], respectively, hydrothermal [50] methods. The structural, optical, surface and photocatalytic properties of CuS/CQD composites and CuS NPs, together with organic pollutant details, are given in Table 2.

Table 2. The structural, optical, surface and photocatalytic properties of CuS NPs and CuS/carbon-based materials composites.

Catalyst	Morphology	Eg (eV)	S_{BET} (m^2/g)	Photodegradation				Ref.
				Dye				
				Chemical Formula and Structure	λ_{max} (nm)	η* (%)	t (min)	
CuS NPs	spherical (10–12 nm)	3.46	9.36	BG, $C_{27}H_{33}N_2.HO_4S$		38		
CuS/CQDs	compact loading of carbon dots (4–8 nm) over CuS NPs	2.96	15.42	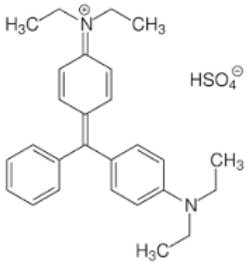	625	91.8	90	[78]
CuS NPs	nano-flower-like structure	-	850.5	PAN, $C_8H_9NO_2$		76.9		
CuS/CQDs	small nano-flowers with nano-petals	-		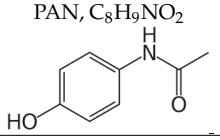	243	96.5	100	[50]
CuS NPs	urchin-like structure and some irregular hexagonal NPs	2.08	20.25	MG, $C_{23}H_{25}ClN_2$		92		
CuS/rGO	uniform CuS NPs distributed on rGO nanosheets	1.9	34.4	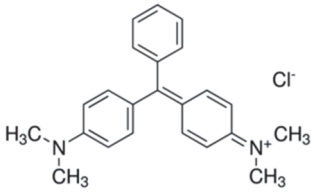	621	99.2	90	[14]
CuS NPs	hexagonal	2.07	130	ATZ, $C_8H_{14}ClN_5$		60	50	
CuS/rGO	separated hexagons of CuS assembled on rGO	1.76	155	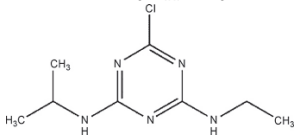	222.5	100	20	[43]

η* is the efficiency degradation of pollutant after t min of irradiation.

Due to improved morphologies, large surface areas and reduced band gap energies, and therefore, superior capacity for light absorption, these composites were shown to be the most effective catalysts for dyes and active pharmaceutical photodegradation. The CuS/CQDs catalyst act as a scavenger during the photocatalytic process, reducing the electron-hole recombination rate, and the possible redox reactions are summarized in Figure 5.

Both CuS/CQDsq photocatalysts were prepared via green techniques, representing an easy and low-cost way to remove organic pollutants and plant waste from the environment (i.e., wastewater).

The photocatalytic performance of CuS/rGO nanocomposites was evaluated for the degradation of toxic persistent organic pollutants, malachite green (MG) and atrazine (ATZ), under direct/simulated sunlight radiance [14,43]. Malachite green is a carcinogenic and non-biodegradable dye used in numerous industrial applications. Atrazine, a commonly used herbicide in the agriculture and food industries, is one of the most stable toxic contaminants in polluted water. The molecular formulae and structures of the organic pollutants, together with the structural, optical, surface and photocatalytic properties of CuS/rGO composites and CuS NPs are presented in Table 2.

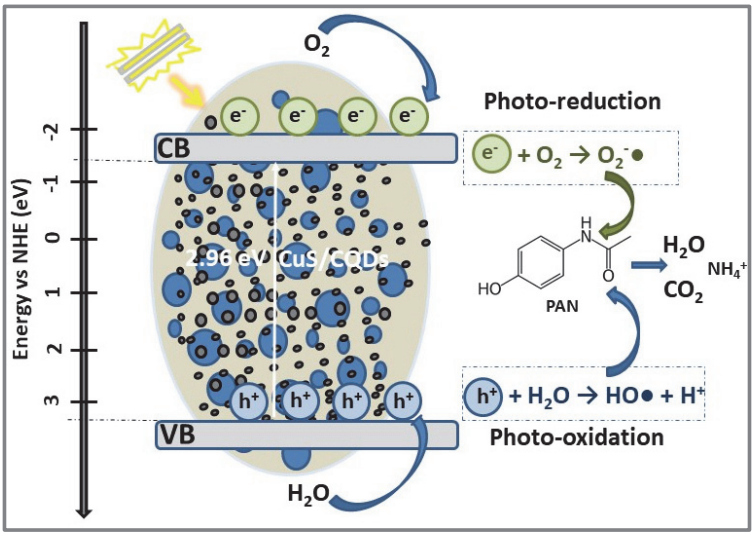

Figure 5. The photocatalytic degradation mechanism of PAN drug using CuS/CQDs photocatalyst under Vis light irradiation (400 W mercury lamp).

The experimental results revealed that the addition of various wt% of rGO in CuS had significant contributions to persistent organic pollutant photodegradation with CuS/rGO composite, such as the following: (a) enhanced light absorption and decreased bandgap energy values from 2.08 eV to 1.76−1.9 eV; (b) ensured relatively large specific surface area which provided more active reaction sites exhibiting strong photo-absorption of pollutant molecules under solar/Vis light irradiations; (c) allowed strong adsorption of pollutant molecules due to the oxygen-containing functional groups on the surface of rGO. The mechanism of ATZ degradation by CuS/rGO photocatalyst is illustrated in Figure 6. The absorption of light photons with energy (hυ) higher than the band gap energy of CuS (Eg = 2.07 eV) generated photo-excited electrons (e^-) on CB, and holes (h^+) in the VB. The rGO nanosheets, which were anchored to the surface of the assembled CuS NPs, could receive the photo-excited e^-, favoring the separation of photogenerated charge carriers and oxidized species (HO·, $\cdot O_2^-$) formation. These active radicals reacted with the ATZ molecules adsorbed on the photocatalyst active sites, resulting in CO_2, H_2O and other non-harmful ions [43].

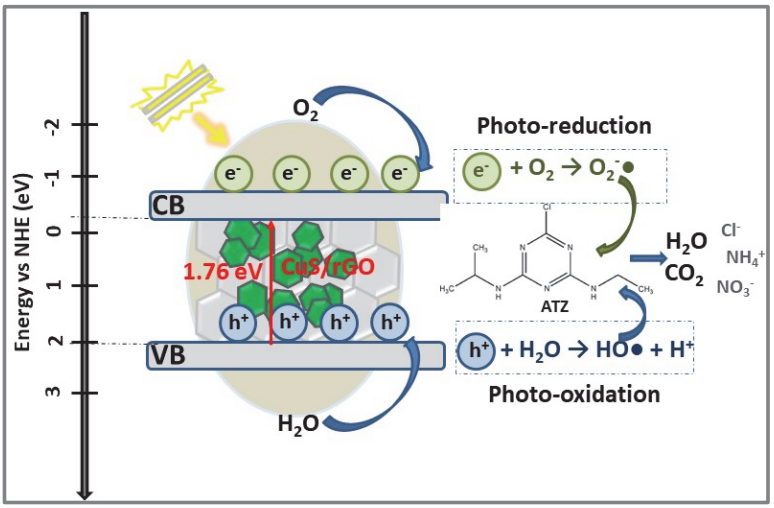

Figure 6. The photocatalytic degradation mechanism of ATZ herbicide using CuS/rGO photocatalyst under Vis light irradiation (300 W Xe lamp with λ < 410 nm cut-off sieve).

The reusability and photo-stability studies showed that CuS/rGO heterojunction nanostructure had the capacity to regenerate several times (e.g., 5 times), without a significant loss in its photodegradation efficiency, therefore exhibiting a high stability under light irradiation [14,43].

3.2. CuS/Organic Semiconductor Heterostructures as Catalysts for Organic Pollutant Photodegradation

PDI, one of the most studied organic fluorescent dyes, has excellent optoelectronic properties, specific to an n-type semiconductor, and, therefore, is used in solar cells and sensor applications. Supramolecular architectures (NS 1D) formed by self-assembled PDI are of particular interest in photocatalytic materials development due to their high photo-thermal stability, charge mobility, and electron affinity [79,82].

A recent study [79] reported the synthesis of a novel CuS/PDI p-n heterojunction photocatalyst for removal of tetracycline (TC) from wastewater. The CuS/PDI composites were prepared using a two-step self-assembly procedure, varying the CuS concentration (5%, 10%, 15%) in self-assembled PDI. By comparison with pure self-assembled PDI and CuS nanosheets, higher efficiency in photodegradation of TC, under simulated visible light, after 2 h, was obtained for the CuS10%/PDI catalyst. Thus, before coupling, both pure CuS (Eg = 2.01 eV, SBET = 1.87 m^2/g) and PDI (Eg = 1.67 eV, SBET = 0.76 m^2/g) catalysts showed poor photocatalytic performance, meaning about 40% and 60%, respectively, within 120 min. After coupling, and p-n heterojunction formation, the CuS/PDI composite (Eg = 1.71 eV, SBET = 39.43 m^2/g) exhibited higher efficiency (about 90%) for TC degradation. The enhancement of CuS/PDI photocatalytic activity was mainly attributed to the highly ordered H-type p-p stacking in the PDI structure and the p-n junction, which allowed the fast separation of the photo-generated charge carrier pairs. After the formation of a p-n junction, the photo-electrons were transferred from CuS CB to self-assembled PDI CB, under the action of the internal electric field, while photo-holes migrated in the opposite direction, from the self-assembled PDI VB to that of CuS. The transferred electrons further reacted with O_2, resulting in peroxide ion radicals $\cdot O_2^-$ and holes, which produced active radicals ·OH after the reaction with H_2O. Both active oxidized radicals acted as reactants in further decomposition of TC on the catalyst surface (Figure 7).

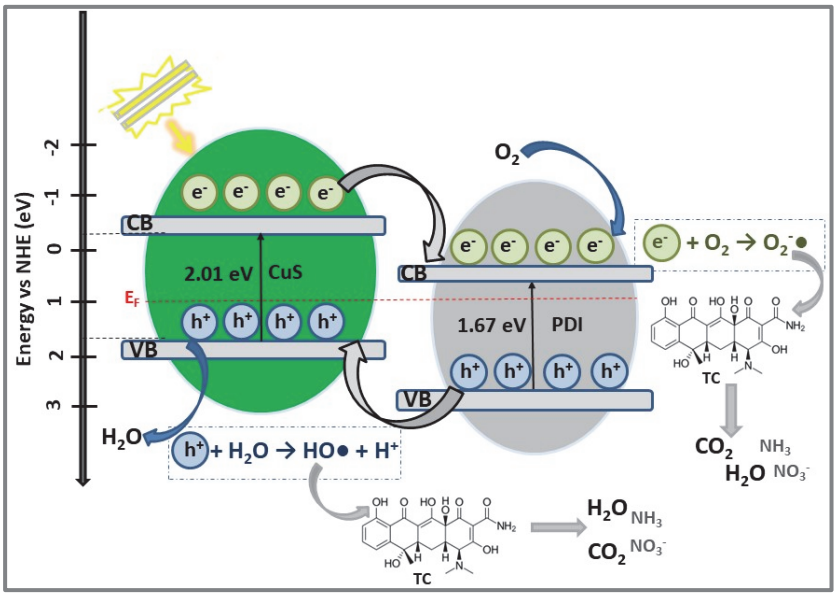

Figure 7. The photocatalytic degradation mechanism of TC antibiotic using CuS/PDI catalyst under Vis light irradiation (300 W Xe lamp with a cut filter with λ > 420 nm).

The stability and reusability experiments encountered some problems with the powder catalyst, therefore PDI/CuS composite was coupled with the modified cotton fibers

through electrostatic adsorption. The newly-designed photocatalytic fabric was tested under simulated actual water quality conditions and, after 5 cycles, the degradation rate was maintained at about 80%, which indicated good reusability [79].

3.3. CuS/Metal Oxide Heterostructures as Catalysts for Organic Pollutant Photodegradation

Wide band gap semiconductors, such as TiO_2 (Eg = 3.25 eV [83]), SnO_2 (Eg = 3.4 eV [84]) and ZnO (Eg = 3.2 eV [85]), perform better as photocatalysts in the UV region, which causes their limited use in industrial applications, and, thus, a significant increase in process costs. Another factor that limits their photocatalytic efficiency is the rapid recombination of charge carriers. To extend the photocatalytic response in the Vis spectral region, and to reduce the recombination processes, many heterojunctions have been developed in recent years by coupling a wide band gap semiconductor with a suitable narrow band gap semiconductor, such as CuS. Most of the previously published review articles on CuS nanostructured materials have focused on synthesis methods, special properties, and prospective applications [28,29,36]. More recently, in a mini-review, we published the developments on dye photodegradation using various copper sulfide-based heterojunctions (copper sulfide/metal oxide, copper sulfide/metal sulfide, copper sulfide/graphene, copper sulfide/organic semiconductors) as catalysts [4].

Recently, Sudhaik et al. [46] published an extensive literature study (review) on CuS and different CuS-based heterostructured materials as photocatalysts for wastewater treatment. Thus, in this part of the article, approaches related to recently developed CuS-based heterojunctions as catalysts for organic pollutant photodegradation are highlighted, issues that were not considered in the previously mentioned publications.

The enhanced visible light photocatalytic efficiency of type II heterojunction CuS/ZnO in MB and toluidine blue (TB) degradation was reported by Khausik B et al. [80]. The CuS/ZnO photocatalyst was obtained by assembling p-type CuS NPs on n-type ZnO heterostructures, using hydrothermal method. For the photocatalysis experiments, 35 mg of CuS/ZnO catalyst and 50 mL aqueous solution of MB (3×10^{-5} M), respectively TB (6×10^{-5} M), were used. The photocatalytic experiments showed that the tandem structure of CuS/ZnO had excellent photocatalytic efficiency for MB and TB, with 93% and 87.5% dyes degradation within 16 respectively 18 min, under visible light irradiation. The remarkable photocatalytic activity was attributed to the CuS/ZnO p-n heterojunction formation, which favored the efficient separation of photoinduced charge carriers.

Based on scavenging experiments using different trappers, the mechanism proposed for the degradation of MB and TB under Vis light corresponds to type II heterojunction CuS-based photocatalyst (Figure 8), allowing the transfer of electrons and holes to the other semiconductor from heterojunction (ZnO), when spatial charge carriers separation occurred.

To summarize, in the photocatalytic degradation of dyes by CuS/ZnO catalyst, the photo-excited electrons and holes generate highly reactive hydroxyl radicals (HO·) which decompose pollutants into CO_2, H_2O and other environmentally friendly compounds that do not require any other chemical or physical treatment.

Recently, WO_3 with activated carbon (AC, 1% and 2%) and co-doped with CuS (10%, 15%) composites, WO_3-AC/CuS, were prepared via a facile hydrothermal method [80].

The hydrothermal method was used because it allows the control of the composite's structural, morphological and optical properties, in order to increase photocatalytic activity, by varying the synthesis parameters, such as temperature and time. The nano-rod-like structure (500 nm with size of nano-rods of 80–89 nm) of WO_3 became sharper and clear after doping with AC and was covered with small nanoflowers of hexagonal CuS in WO_3-AC/CuS composites. This morphology demonstrated itself to be suitable for the degradation of organic pollutants, in this case aspirin. In addition, the UV–Vis analysis results showed that increasing the AC and CuS amounts in WO_3 caused the bandgap energy to decrease from 2.49 eV (WO_3) to 2.3 eV (WO_3-2% AC), and to 1.92 eV for WO_3-2% AC/15% CuS. This reduction of band-gap energy confirmed that the addition of CuS enhanced the optical properties, and, therefore, the photocatalytic performance of WO_3-Ac material.

The photocatalytic experiments were focused on the comparative degradation of aspirin (10 mg/L), as an active pharmaceutical contaminant model, under Vis light (home-made photocatalytic reactor with a 400 W metal halide lamp) in the presence of catalysts WO_3, WO_3-AC and WO_3-AC/CuS.

The results showed that ASP photodegradation increased from 40% (WO_3) to 97.6% when WO_3-AC/CuS heterostructure was used as catalyst, after 150 min of Vis light illumination. This high photocatalytic activity was due to the increase of the photo-generated charges recombination ratio and the decrease of the photon depth penetration. The proposed mechanism for the degradation of ASP by WO_3-AC/CuS photocatalyst is schematically presented in Figure 9.

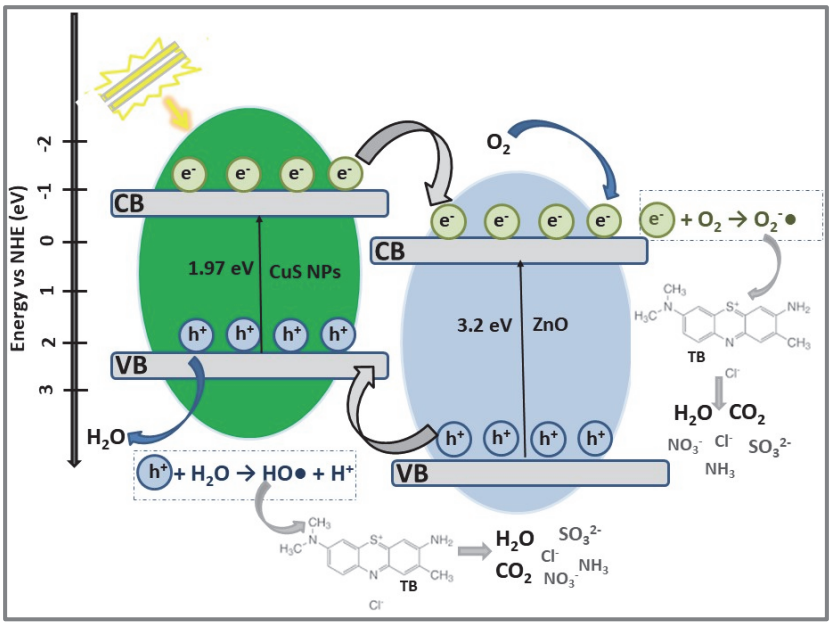

Figure 8. The photocatalytic degradation mechanism of toluidine blue (TB) dye using CuS/ZnO catalyst under Vis light irradiation.

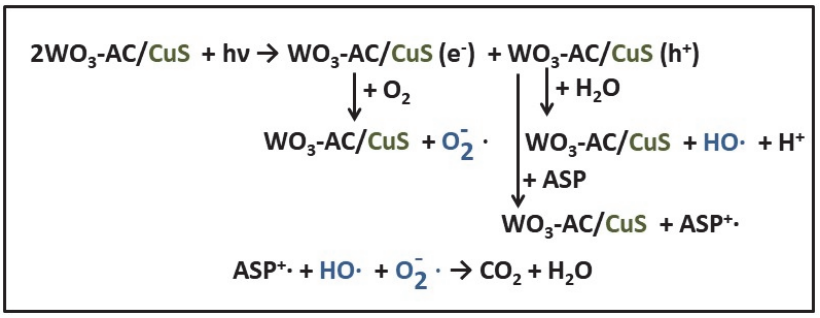

Figure 9. The reaction mechanism for ASP photodegradation by WO_3-AC/CuS catalyst.

4. Conclusions

Covellite (CuS), a p-type semiconductor, is a promising Vis light-responsive photocatalyst due to its narrow bandgap (Eg = 1.7–2.2 eV) and good optical absorption properties in the Vis to NIR region. In this review, the influence of different CuS properties (morphology, particle size, bandgap energy, and surface properties) and synthesis parameters (Cu:S molar ratios, precursor concentration, surfactant amount in precursors solutions, etc.) on the photocatalytic activity of CuS-based catalysts (CuS nanostructures and CuS-based heterostructures) for various toxic, non-biodegradable, and recalcitrant organic pollutants (dyes, herbicides, active pharmaceuticals compounds) degradation was discussed.

Photocatalytic performances of CuS nanostructures and CuS-based heterostructures in organic pollutants removal from wastewater contribute to the further development of various CuS-based photocatalysts with enhanced solar energy conversion efficiency for environmental remediation and green energy production.

Author Contributions: Conceptualization, L.I; methodology, L.I.; literature investigation, L.I., C.C., L.A. and A.E.; writing—original draft preparation, L.I.; writing—review and editing, L.I. and A.E.; visualization, L.I., C.C., L.A. and A.E.; supervision, A.E. All authors have read and agreed to the published version of the manuscript.

Funding: This work was supported by a grant of the Ministry of Research, Innovation, and Digitization, CNCS–UEFISCDI, project number PN-III-P4-PCE-2021-1020 (PCE87), within PNCDI III.

Conflicts of Interest: The authors declare no conflict of interest.

Abbreviations

MCs	microcrystals
HT	hydrothermal
ST	solvothermal
SG	sol–gel
CoPp	Co-precipitation
MV	methyl violet
MG	malachite green
MO	methyl orange
EY	eosin Y
CR	congo red
MoO	mordant orange
SO	safranine orange
AO	acridine orange
ABRX-3B	active brilliant red X-3B
4-CP	4-chlorophenol
HA	humic acid
ASP	aspirin
S-MCh	S-metolachlor
PVP	polyvinylpyrrolidone
KCC1	Fibrous silica KAUST Catalysis Centre
MAA	methacrylic acid
PDI	perylene diimide
CB	conduction band
VB	valence band

References

1. Xu, G.; Du, M.; Zhang, J.; Li, T.; Guan, Y.; Guo, C. Facile fabrication of magnetically recyclable $Fe_3O_4/BiVO_4/CuS$ heterojunction photocatalyst for boosting simultaneous Cr(VI) reduction. *J. Alloys Compd.* **2022**, *895*, 162631. [CrossRef]
2. Li, Z.; Menga, X.; Zhang, Z. Recent development on MoS_2-based photocatalysis: A review. *J. Photochem. Photobiol. C Photochem. Rev.* **2018**, *35*, 39–55. [CrossRef]
3. Jiang, N.; Du, Y.; Ji, P.; Liu, S.; He, B.; Qu, B.; Wang, J.; Suna, X. Enhanced photocatalytic activity of novel $TiO_2/Ag/MoS_2/Ag$ nanocomposites for water-treatment. *Ceram. Int.* **2020**, *46*, 4889–4896. [CrossRef]
4. Isac, L.; Cazan, C.; Enesca, A.; Andronic, A. Copper Sulfide Based Heterojunctions as Photocatalysts for Dyes Photodegradation. *Front. Chem.* **2019**, *7*, 694. [CrossRef]
5. Jabbar, Z.H.; Graimed, B.H. Recent developments in industrial organic degradation via semiconductor heterojunctions and the parameters affecting the photocatalytic process: A review study. *J. Water Process. Eng.* **2022**, *47*, 102671. [CrossRef]
6. El-Hakam, S.A.; Alshorifi, F.T.; Salama, R.S.; Gamal, S.; Abo El-Yazeed, W.S.; Ibrahim, A.A.; Ahmed, A.I. Application of nanostructured mesoporous silica/bismuth vanadate composite catalysts for the degradation of methylene blue and brilliant green. *J. Mater. Res. Technol.* **2022**, *18*, 1963–1976. [CrossRef]
7. Alshorifi, F.T.; Abduliah, A.A.; Salama, R.S. Gold-selenide quantum dots supported onto cesium ferrite nanocomposites for the efficient degradation of rhodamine B. *Helyon* **2022**, *8*, E09652. [CrossRef] [PubMed]

8. Huang, X.; Chen, C.; Tsai, H.; Shaya, J.; Lu, C. Photocatalytic degradation of thiobencarb by a visible light-driven MoS_2 photocatalyst. *Sep. Purif. Technol.* **2018**, *197*, 147–155. [CrossRef]
9. Prabhakar Vattikuti, S.V.; Shim, J. Synthesis, characterization and photocatalytic performance of chemically exfoliated MoS_2. *IOP Conf. Ser. Mater. Sci. Eng.* **2018**, *317*, 012025. [CrossRef]
10. Sivaranjani, P.R.; Janani, B.; Thomas, A.M.; Raju, L.L.; Khan, S.S. Recent development in MoS_2-based nano-photocatalyst for the degradation of pharmaceutically active compounds. *J. Clean. Prod.* **2022**, *352*, 131506. [CrossRef]
11. Wang, W.; Liu, Y.; Yu, S.; Wen, X.; Wu, D. Highly efficient solar-light-driven photocatalytic degradation of pollutants in petroleum refinery wastewater on hierarchically-structured copper sulfide (CuS) hollow nanocatalysts. *Sep. Purif. Technol.* **2022**, *284*, 120254. [CrossRef]
12. Vaiano, V.; Sacco, O.; Barba, D.; Palma, V. Zinc Sulfide Prepared through ZnO Sulfuration: Characterization and Photocatalytic Activity. *Chem. Eng. Trans.* **2019**, *74*, 1159–1164. [CrossRef]
13. Ikram, M.; Khan, M.I.; Raza, A.; Imran, M.; Ul-Hamid, A.; Ali, S. Outstanding performance of silver-decorated MoS_2 nanopetals used as nanocatalyst for synthetic dye degradation. *Phys. E Low-Dimens. Syst. Nanostruct.* **2020**, *124*, 114126. [CrossRef]
14. El-Hout, S.I.; El-Sheikh, S.M.; Gaber, A.; Shawky, A.; Ahmed, A.I. Highly efficient sunlight-driven photocatalytic degradation of malachite green dye over reduced graphene oxide-supported CuS nanoparticles. *J. Alloys Compd.* **2020**, *849*, 156573. [CrossRef]
15. Sabbah, A.; Shown, I.; Qorbani, M.; Fu, F.-Y.; Lin, T.-Y.; Wu, H.-L.; Chung, P.-W.; Wu, C.-Y.; Santiago, S.R.M.; Shen, J.-L.; et al. Boosting photocatalytic CO_2 reduction in a $ZnS/ZnIn_2S_4$ heterostructure through strain-induced direct Z-scheme and a mechanistic study of molecular CO_2 interaction thereon. *Nano Energy* **2022**, *93*, 106809. [CrossRef]
16. He, R.-M.; Yang, Y.-L.; Chen, H.-J.; Liu, J.-J.; Sun, Y.-M.; Guo, W.-N.; Li, D.-H.; Hou, X.-J.; Suo, G.-Q.; Ye, X.-H.; et al. In situ controllable growth of Cu_7S_4 nanosheets on copper mesh for catalysis: The synergistic effect of photocatalytic Fenton-like process. *Colloids Surf. A Physicochem. Eng. Asp.* **2022**, *642*, 128651. [CrossRef]
17. Jiang, G.; Zhu, B.; Sun, J.; Liu, F.; Wang, Y.; Zhao, C. Enhanced activity of ZnS (111) by N/Cu co-doping: Accelerated degradation of organic pollutants under visible light. *J. Environ. Sci.* **2023**, *125*, 244–257. [CrossRef]
18. Mouchaal, Y.; Enesca, A.; Mihoreanu, C.; Khelil, A.; Duta, A. Tuning the opto-electrical properties of SnO_2 thin films by Ag^{+1} and In^{+3} co-doping. *Mater. Sci. Eng. B* **2015**, *199*, 22–29. [CrossRef]
19. Yang, F.; Zhang, Z.; Wang, Y.; Xu, M.; Zhao, W.; Yan, J.; Chen, C. Facile synthesis of nano-MoS_2 and its visible light photocatalytic property. *Mater. Res. Bull.* **2017**, *87*, 119–122. [CrossRef]
20. Dudita, M.; Bogatu, C.; Enesca, A.; Duta, A. The influence of the additives composition and concentration on the properties of SnO_x thin films used in photocatalysis. *Mater. Lett.* **2011**, *65*, 2185–2189. [CrossRef]
21. Hamida, A.A.; Al-Maiyaly, B.K.H. Synthesis and characterization of Cu_2S:Al thin films for solar cell applications. *Chalcogenide Lett.* **2022**, *19*, 579–590. [CrossRef]
22. Wong, A.B.; Brittman, S.; Yu, Y.; Dasgupta, N.P.; Yang, P. Core-Shell CdS-Cu_2S Nanorod Array Solar Cells. *Nano Lett.* **2015**, *15*, 4096–4101. [CrossRef] [PubMed]
23. Wen, L.; Chen, Q.; Zhou, L.; Huang, M.; Lu, J.; Zhong, X.; Fan, H.; Ou, Y. $Cu_{1.8}S$@CuS composite material improved the photoelectric efficiency of cadmium-series QDSSCs. *Opt. Mater.* **2020**, *108*, 110172. [CrossRef]
24. Peng, M.; Ma, L.-L.; Zhang, Y.-G.; Tan, M.; Yu, Y. Controllable synthesis of self-assembled Cu_2S nanostructures through a template-free polyol process for the degradation of organic pollutant under visible light. *Mater. Res. Bull.* **2009**, *44*, 1834–1841. [CrossRef]
25. Enesca, A.; Isac, L. Tuned S-Scheme $Cu_2S\_TiO_2\_WO_3$ Heterostructure Photocatalyst toward S-Metolachlor (S-MCh) Herbicide Removal. *Materials* **2021**, *14*, 2231. [CrossRef]
26. Li, S.; Zhang, Z.; Yan, L.; Jiang, S.; Zhu, N.; Li, J.; Li, W.; Yu, S. Fast synthesis of CuS and Cu_9S_5 microcrystal using subcritical and supercritical methanol and their application in photocatalytic degradation of dye in water. *J. Supercrit. Fluids.* **2017**, *123*, 11–17. [CrossRef]
27. Isac, L.; Nicoara, L.; Panait, R.; Enesca, A.; Perniu, D.; Duta, A. Alumina matrix with controlled morphology for colored spectrally selective coatings. *Environ. Eng. Manag. J.* **2017**, *16*, 715–724. [CrossRef]
28. Nemade, K.R.; Waghuley, S.A. Band gap engineering of CuS nanoparticles for artificial photosynthesis. *Mater. Sci. Semicond. Process.* **2015**, *39*, 781–785. [CrossRef]
29. Shamraiz, U.; Hussain, R.A.; Badshah, A. Fabrication and applications of copper sulfide (CuS) nanostructures. *J. Solid State Chem.* **2016**, *238*, 25–40. [CrossRef]
30. Mohamed, E.F.; Dob, T.-O. Synthesis of New Hollow Nanocomposite Photocatalysts: Sunlight Applications for Removal of Gaseous Organic Pollutants. *J. Taiwan Inst. Chem. Eng.* **2020**, *111*, 181–190. [CrossRef]
31. Borthakur, P.; Boruah, P.K.; Das, M.R. Facile synthesis of CuS nanoparticles on two-dimensional nanosheets as efficient artificial nanozyme for detection of Ibuprofen in water. *J. Environ. Chem. Eng.* **2021**, *9*, 104635. [CrossRef]
32. Arshad, M.; Wang, Z.; Nasir, J.A.; Amador, E.; Jin, M.; Li, H.; Chen, Z.; Rehman, Z.; Chen, W. Single source precursor synthesized CuS nanoparticles for NIR phototherapy of cancer and photodegradation of organic carcinogen. *J. Photochem. Photobiol. B Biol.* **2021**, *214*, 112084. [CrossRef] [PubMed]
33. Kaur, A.; Singh, K. Investigation of crystalographic, morphological and photocatalytic behaviour of Ag doped CuS nanostructures. *Mater. Today Proc.* **2022**, *60*, 1090–1098. [CrossRef]

34. Goel, S.; Chen, F.; Cai, W. Synthesis and Biomedical Applications of Copper Sulfide Nanoparticles: From Sensors to Theranostics. *Small* **2014**, *10*, 631–645. [CrossRef] [PubMed]
35. Jiang, K.; Chen, Z.; Meng, X. CuS and Cu_2S as Cathode Materials for Lithium Batteries: A Review. *ChemElectroChem* **2019**, *6*, 28243. [CrossRef]
36. Majumdar, D. Recent progress in copper sulfide based nanomaterials for high energy supercapacitor applications. *J. Electroanal. Chem.* **2021**, *880*, 114825. [CrossRef]
37. Yu, B.; Meng, F.; Zhou, T.; Fan, A.; Khan, M.W.; Wu, H.; Liu, X. Construction of hollow TiO_2/CuS nanoboxes for boosting full-spectrum driven photocatalytic hydrogen evolution and environmental remediation. *Ceram. Int.* **2021**, *47*, 8849–8858. [CrossRef]
38. Mutalik, C.; Okoro, G.; Krisnawati, D.I.; Jazidie, A.; Rahmawati, E.Q.; Rahayu, D.; Hsu, W.-T.; Kuo, T.-R. Copper sulfide with morphology-dependent photodynamic and photothermal antibacterial activities. *J. Colloid Interface Sci.* **2022**, *607*, 1825–1835. [CrossRef]
39. Ding, H.; Han, D.; Hana, Y.; Liang, Y.; Liu, X.; Li, Z.; Zhu, S.; Wu, S. Visible light responsive CuS/protonated g-C3N4 heterostructure for rapid sterilization. *J. Hazard. Mater.* **2020**, *393*, 122423. [CrossRef]
40. Zhang, Z.; Sun, Y.; Mo, S.; Kim, J.; Guo, D.; Ju, J.; Yu, J.; Liu, M. Constructing a highly efficient CuS/Cu_9S_5 heterojunction with boosted interfacial charge transfer for near-infrared photocatalytic disinfection. *Chem. Eng. J.* **2022**, *431*, 134287. [CrossRef]
41. Agboola, P.O.; Haider, S.; Shakir, I. Copper sulfide and their hybrids with carbon nanotubes for photocatalysis and antibacterial studies. *Ceram. Int.* **2022**, *48*, 10136–10143. [CrossRef]
42. Chang, C.-J.; Lin, Y.-G.; Chen, J.; Huang, C.-Y.; Hsieh, S.-C.; Wu, S.-Y. Ionic liquid/surfactant-hydrothermal synthesis of dendritic PbS@CuS core-shell photocatalysts with improved photocatalytic performance. *Appl. Surf. Sci.* **2021**, *546*, 149106. [CrossRef]
43. Alhaddad, M.; Shawky, A. CuS assembled rGO heterojunctions for superior photooxidation of atrazine under visible light. *J. Mol. Liq.* **2020**, *318*, 114377. [CrossRef]
44. Enesca, A.; Duta, A. Tailoring WO_3 thin layers using spray pyrolysis technique. *Phys. Status Solidi C* **2008**, *5*, 3499–3502. [CrossRef]
45. Morales-García, A.; Soares, A.L., Jr.; Dos Santos, E.C.; de Abreu, H.A.; Duarte, H.A. First-Principles Calculations and Electron Density Topological Analysis of Covellite (CuS). *J. Phys. Chem. A* **2014**, *118*, 5823–5831. [CrossRef] [PubMed]
46. Sudhaik, A.; Raizada, P.; Rangabhashiyam, S.; Singh, A.; Nguyen, V.-H.; Le, Q.V.; Khan, A.A.P.; Hu, C.; Huang, C.-W.; Ahamad, T.; et al. Copper sulfides based photocatalysts for degradation of environmental pollution hazards: A review on the recent catalyst design concepts and future perspectives. *Surf. Interfaces* **2022**, *33*, 102182. [CrossRef]
47. Deng, J.; Zhao, Z.-Y. Effects of non-stoichiometry on electronic structure of Cu_xS_y compounds studied by first-principle calculations. *Mater. Res. Express* **2019**, *6*, 105513. [CrossRef]
48. Kalanur, S.S.; Seo, H. Tuning plasmonic properties of CuS thin films via valence band filling. *RSC Adv.* **2017**, *7*, 11118–11122. [CrossRef]
49. Yooa, J.-H.; Ji, M.; Kim, J.H.; Ryu, C.-H.; Lee, Y.-I. Facile synthesis of hierarchical CuS microspheres with high visible-light driven photocatalytic activity. *J. Photochem. Photobiol. A Chem.* **2020**, *401*, 112782. [CrossRef]
50. Iqbal, T.; Ashraf, M.; Afsheen, S.; Masood, A.; Qureshi, M.T.; Obediat, S.T.; Hamed, M.F.; Othman, M.S. Copper sulfide (CuS) doped with carbon quantum dots (CQD) as an efficient photocatalyst. *Opt. Mater.* **2022**, *125*, 112116. [CrossRef]
51. Li, Y.-H.; Wang, Z. Green synthesis of multifunctional copper sulfide for efficient adsorption and photocatalysis. *Chem. Zvesti.* **2019**, *73*, 2297–2308. [CrossRef]
52. Wu, H.; Li, Y.; Li, Q. Facile synthesis of CuS nanostructured flowers and their visible light photocatalytic properties. *Appl. Phys. A* **2017**, *123*, 196. [CrossRef]
53. Tanveer, M.; Cao, C.; Ali, Z.; Aslam, I.; Idrees, F.; Khan, W.S.; But, F.K.; Tahir, M.; Mahmood, N. Template free synthesis of CuS nanosheet-based hierarchical microspheres: An efficient natural light driven photocatalyst. *CrystEngComm* **2014**, *16*, 5290–5300. [CrossRef]
54. Ain, N.; Rehman, Z.; Aamir, A.; Khan, Y.; Rehman, M.; Lin, D.-J. Catalytic and photocatalytic efficacy of hexagonal CuS nanoplates derived from copper(II) dithiocarbamate. *Mater. Chem. Phys.* **2020**, *242*, 1224078. [CrossRef]
55. Nancucheo, A.; Segura, A.; Hernandez, P.; Hernandez-Montelongo, J.; Pesenti, H.; Arranz, A.; Benito, N.; Romero-Saez, M.; Contreras, B.; Díaz, V.; et al. Covellite nanoparticles with high photocatalytic activity bioproduced by using H_2S generated from a sulfidogenic bioreactor. *J. Environ. Chem. Eng.* **2022**, *10*, 107409. [CrossRef]
56. Jiang, J.; Jiang, Q.; Deng, R.; Xie, X.; Meng, J. Controllable preparation, formation mechanism and photocatalytic performance of copper base sulfide nanoparticles. *Mater. Chem. Phys.* **2020**, *254*, 123504. [CrossRef]
57. Adhikari, S.; Sarkar, D.; Madras, G. Hierarchical Design of CuS Architectures for Visible Light Photocatalysis of 4-Chlorophenol. *ACS Omega* **2017**, *2*, 4009–4021. [CrossRef]
58. Bhatt, V.; Kumar, M.; Yun, J.-H. Unraveling the photoconduction characteristics of single-step synthesized CuS and Cu_9S_5 micro-flowers. *J. Alloys Compd.* **2021**, *891*, 161940. [CrossRef]
59. Fang, J.; Zhang, P.; Chang, Z.; Wang, X. Hydrothermal synthesis of nanostructured CuS for broadband efficient optical absorption and high-performance photo-thermal conversion. *Sol. Energy Mater. Sol. Cells* **2018**, *185*, 456–463. [CrossRef]
60. Yan, X.; Michael, E.; Komarneni, S.; Brownson, J.R.; Yan, Z.-F. Microwave- and conventional-hydrothermal synthesis of CuS, SnS and ZnS: Optical properties. *Ceram. Int.* **2013**, *39*, 4757–4763. [CrossRef]

61. Ayodhya, D.; Venkatesham, M.; Kumari, A.S.; Reddy, G.B.; Ramakrishna, D.; Veerabhadram, G. Photocatalytic degradation of dye pollutants under solar, visible and UV lights using green synthesised CuS nanoparticles. *J. Exp. Nanosci.* **2016**, *11*, 418–432. [CrossRef]
62. Wang, X.; He, Y.; Hu, Y.; Jin, G.; Jiang, B.; Huang, Y. Photothermal-conversion-enhanced photocatalytic activity of flower-like CuS superparticles under solar light irradiation. *Sol. Energy* **2018**, *170*, 586–593. [CrossRef]
63. Saranya, M.; Ramachandran, R.; Samuel, E.J.; Jeong, S.K.; Grace, A.N. Enhanced visible light photocatalytic reduction of organic pollutant and electrochemical properties of CuS catalyst. *Powder Technol.* **2014**, *252*, 25–32. [CrossRef]
64. Iqbal, S.; Shaid, N.A.; Sajid, M.M.; Javed, Y.; Fakhar-e-Alam, M.; Mahmood, A.; Ahmad, G.; Afzal, A.M.; Hussain, S.Z.; Ali, F.; et al. Extensive evaluation of changes in structural, chemical and thermal properties of copper sulfide nanoparticles at different calcination temperature. *J. Cryst. Growth* **2020**, *547*, 125823. [CrossRef]
65. Pejjai, B.; Reddivari, M.; Kotte, T.R.R. Phase controllable synthesis of CuS nanoparticles by chemical co-precipitation method: Effect of copper precursors on the properties of CuS. *Mater. Chem. Phys.* **2020**, *239*, 122030. [CrossRef]
66. Andronic, L.; Isac, L.; Cazan, C.; Enesca, A. Simultaneous Adsorption and Photocatalysis Processes Based on Ternary TiO_2–Cu_xS–Fly Ash Hetero-Structures. *Appl. Sci.* **2020**, *10*, 8070. [CrossRef]
67. Li, S.; Ge, Z.-G.; Zhang, Z.-P.; Yao, Y.; Wang, H.-C.; Yang, J.; Li, Y.; Gao, G.; Lin, Y.-H. Mechanochemically synthesized sub-5 nm sized CuS quantum dots with high visible-light-driven photocatalytic activity. *Appl. Surf. Sci.* **2016**, *384*, 272–278. [CrossRef]
68. Balaz, M.; Dutkov, E.; Bujnakova, Z.; Tothova, E.; Kostova, N.G.; Karakirova, Y.; Briancin, J.; Kanuchov, M. Mechanochemistry of copper sulfides: Characterization, surface oxidation and photocatalytic activity. *J. Alloys Compd.* **2018**, *746*, 576–582. [CrossRef]
69. Shamraiz, U.; Badshah, A.; Hussain, R.A.; Nadeem, M.A.; Sab, S. Surfactant free fabrication of copper sulphide (CuS–Cu_2S) nanoparticles from single source precursor for photocatalytic applications. *J. Saudi Chem. Soc.* **2017**, *21*, 390–398. [CrossRef]
70. Cruz, J.S.; Hernández, S.A.M.; Delgado, F.P.; Angel, O.Z.; Pérez, R.C.; Delgado, G.T. Optical and Electrical Properties of Thin Films of CuS Nanodisks Ensembles Annealed in a Vacuum and Their Photocatalytic Activity. *Int. J. Photoenergy* **2013**, *2013*, 178017. [CrossRef]
71. Siddique, F.; Rafiq, M.A.; Afsar, M.F.; Hasan, M.M.; Chaudhry, M.M. Enhancement of degradation of mordant orange, safranin-O and acridine orange by CuS nanoparticles in the presence of H_2O_2 in dark and in ambient light. *J. Mater. Sci. Mater. Electron.* **2018**, *29*, 19180–19191. [CrossRef]
72. Hu, X.-S.; Shen, Y.; Xu, L.-H.; Wang, L.-M.; Xing, Y.-J. Preparation of flower-like CuS by solvothermal method and its photodegradation and UV protection. *J. Alloys Compd.* **2016**, *674*, 289–294. [CrossRef]
73. Nabi, G.; Tanveer, M.; Tahir, M.B.; Kiran, M.; Rafique, M.; Khalid, N.R.; Alzaid, M.; Fatima, N.; Nawaz, T. Mixed solvent based surface modification of CuS nanostructures for an excellent photocatalytic application. *Inorg. Chem. Commun.* **2020**, *121*, 108205. [CrossRef]
74. Chai, Z.; Pan, X.; Cui, F.; Ma, Q.; Zhang, J.; Liu, M.; Chen, Y.; Li, L.; Cui, T. Synthesis of 3D hierarchical CuS architectures consisting of 1D nanotubes for efficient photocatalysts. *Mater. Lett.* **2020**, *275*, 128168. [CrossRef]
75. Qin, N.; Wei, W.; Huang, C.; Mi, L. An efficient strategy for the fabrication of CuS as a highly excellent and recyclable photocatalyst for the degradation of organic dyes. *Catalysts* **2020**, *10*, 40. [CrossRef]
76. Mohammadi, N.; Allahresani, A.; Naghizadeh, A. Enhanced photo-catalytic degradation of natural organic matters (NOMs) with a novel fibrous silica-copper sulfide nanocomposite (KCC1-CuS). *J. Mol. Struct.* **2022**, *1249*, 131624. [CrossRef]
77. Kaushik, B.; Yadav, S.; Rana, P.; Solanki, K.; Rawat, D.; Sharma, R.K. Precisely engineered type II ZnO-CuS based heterostructure: A visible light driven photocatalyst for efficient mineralization of organic dyes. *Appl. Surf. Sci.* **2022**, *590*, 153053. [CrossRef]
78. Vyas, Y.; Chundawat, P.; Dharmendra, D.; Jain, A.; Punjabi, P.B.; Ameta, C. Biosynthesis and characterization of carbon quantum Dots@CuS composite using water hyacinth leaves and its usage in photocatalytic dilapidation of Brilliant Green dye. *Mater. Chem. Phys.* **2022**, *281*, 125921. [CrossRef]
79. Yan, L.; Wang, W.; Zhao, Q.; Zhu, Z.; Liu, B.; Hua, C. Construction of perylene diimide/CuS supramolecular heterojunction for the highly efficient visible light-driven environmental remediation. *J. Colloid Interface Sci.* **2022**, *606*, 898–911. [CrossRef]
80. Iqbal, T.; Ashraf, M.; Masood, A. Simple synthesis of WO_3 based activated carbon co-doped CuS composites for photocatalytic applications. *Inorg. Chem. Commun.* **2022**, *139*, 109322. [CrossRef]
81. Baneto, M.; Enesca, A.; Mihoreanu, C.; Lare, Y.; Jondo, K.; Napo, K.; Duta, A. Effects of the growth temperature on the properties of spray deposited $CuInS_2$ thin films for photovoltaic applications. *Ceram. Int.* **2015**, *41*, 4742–4749. [CrossRef]
82. Zhang, F.; Ma, Y.; Chi, y.; Yu, H.; Li, Y.; Jiang, T.; Wei, X.; Shi, J. Self-assembly, optical and electrical properties of perylene diimide dyes bearing unsymmetrical substituents at bay position. *Sci. Rep.* **2018**, *8*, 8208. [CrossRef]
83. Tuckute, S.; Varnagiris, S.; Urbonavicius, M.; Lelis, M.; Sakalauskaite, S. Tailoring of TiO_2 film crystal texture for higher photocatalysis efficiency. *Appl. Surf. Sci.* **2019**, *489*, 576–583. [CrossRef]
84. Aslam, M.; Qamar, M.T.; Ali, S.; Rehman, A.U.; Soomro, M.T.; Ahmed, I.; Ismail, I.M.I.; Hameed, A. Evaluation of SnO_2 for sunlight photocatalytic decontamination of Water. *J. Environ. Manag.* **2018**, *217*, 805–814. [CrossRef]
85. Chen, W.; Liu, Q.; Tian, S.; Zhao, X. Exposed facet dependent stability of ZnO micro/nano crystals as a photocatalyst. *Appl. Surf. Sci.* **2019**, *470*, 807–816. [CrossRef]